International Journal of Geo-Information

MDPI

Article

A Dynamic Algorithm for Measuring Pedestrian Congestion and Safety in Urban Alleyways

Jiyoon Lee [1] and Youngok Kang [1,2,*]

[1] Department of Big Data Analytics, Ewha Womans University, Seoul 03760, Republic of Korea; jiyoon821@ewha.ac.kr
[2] Department of Social Studies (Geography), Ewha Womans University, Seoul 03760, Republic of Korea
* Correspondence: ykang@ewha.ac.kr; Tel.: +82-(2)3277-6646

Abstract: This study presents an algorithm for measuring Pedestrian Congestion and Safety on alleyways, wherein pedestrians and vehicles share limited space, making traditional pedestrian density metrics inadequate. The primary objective is to provide a more accurate assessment of congestion and safety in these shared spaces by incorporating both pedestrian and vehicle interactions, unlike traditional methods that focus solely on pedestrians, regardless of road type. Pedestrian Congestion was calculated using Time to Collision (TTC)-based safety occupation areas, while Pedestrian Safety was assessed by accounting for both physical and psychological safety through proxemics, which measures personal space violations. The algorithm dynamically adapts to changing vehicle and pedestrian movements, providing a more accurate assessment of congestion compared to existing methods. Statistical validation through *t*-tests and K-S (Kolmogorov–Smirnov) tests confirmed significant differences between the proposed method and traditional pedestrian density metrics, while Bland–Altman analysis demonstrated agreement between the two methods. The experimental results reveal that Pedestrian Congestion and Safety varied with time and location, capturing the spatio-temporal characteristics of alleyways. Visual comparisons of Pedestrian Congestion, Safety, and Density further validated that the proposed algorithm provides a more accurate reflection of real-world conditions compared to traditional pedestrian density metrics. These findings highlight the algorithm's ability to measure real-time changes in congestion and safety, incorporate psychological discomfort into safety calculations, and offer a comprehensive analysis by considering both pedestrian and vehicle interactions.

Keywords: pedestrian congestion; pedestrian safety; occupancy space; alleyways; time to collision

check for updates

Citation: Lee, J.; Kang, Y. A Dynamic Algorithm for Measuring Pedestrian Congestion and Safety in Urban Alleyways. *ISPRS Int. J. Geo-Inf.* **2024**, *13*, 434. https://doi.org/10.3390/ijgi13120434

Academic Editors: Zhihua Zhang, M. James C. Crabbe and Wolfgang Kainz

Received: 4 October 2024
Revised: 29 November 2024
Accepted: 30 November 2024
Published: 2 December 2024
Corrected: 11 February 2025

Copyright: © 2024 by the authors. Published by MDPI on behalf of the International Society for Photogrammetry and Remote Sensing. Licensee MDPI, Basel, Switzerland. This article is an open access article distributed under the terms and conditions of the Creative Commons Attribution (CC BY) license (https://creativecommons.org/licenses/by/4.0/).

1. Introduction

In modern urban environments, roads serve as the most critical infrastructure for the movement of both pedestrians and vehicles, making the monitoring and assessment of road congestion and safety a crucial area of research. Numerous studies have been conducted on road congestion, primarily focusing on the calculation of congestion levels and the evaluation of service quality for motor vehicles. These studies typically assess congestion based on vehicle occupancy, travel time, speed, and acceleration [1–5]. Additionally, pedestrian congestion has been studied using pedestrian speed, direction, and turning angle [6–8], or by calculating the pedestrian area occupancy [9,10]. Other studies have measured road saturation by analyzing the density of both pedestrians and vehicles [11–15].

In early research on service levels for pedestrian pathways, Fruin [16] proposed a method to assess pedestrian service levels based on the space occupied per pedestrian, a method still widely referenced today. *The Highway Capacity Manual* in the United States also presents criteria for measuring pedestrian service levels by combining average walking speed and pedestrian occupancy with sidewalk area to evaluate the overall service quality [17]. Most studies evaluating road congestion or service levels have either focused on

vehicles or pedestrians in isolation. However, in mixed-traffic roads where pedestrians and vehicles share the same space, such as backstreets or alleyways, the traditional approaches face significant limitations in representing actual congestion and safety levels. In these contexts, the risk of accidents is particularly high. For instance, a study by a Korean traffic safety institute reported that, from 2013 to 2016, the average number of pedestrian fatalities per year was 7015, of which 5252 (74.9%) occurred on such mixed-use roads [18]. According to the Ministry of Land, Infrastructure, and Transport of the Republic of Korea, 67% of roads in South Korea are classified as backstreets or alleyways. This highlights the need for a new approach to measuring congestion and safety in such environments, distinct from methods used for roads where pedestrians and vehicles are separated.

Given this context, the objective of this study is to develop an algorithm for measuring pedestrian congestion and safety in mixed-use backstreets. Section 2 reviews the relevant literature on pedestrian congestion, while Section 3 details the development of the proposed algorithm for calculating pedestrian congestion and safety. In Section 4, the algorithm is applied to real-world data to assess congestion and safety levels, analyze spatial characteristics of the study area, and compare the algorithm's performance with existing pedestrian service level measurement methods. Finally, Section 5 discusses the significance of the study and future research directions.

This study distinguishes itself from previous research in three significant ways. First, it calculates pedestrian congestion on backstreets by simultaneously accounting for the movement characteristics of both pedestrians and vehicles, including speed, acceleration, inter-object distance, and the safety buffer between them. Second, the safety buffer is not determined by a static snapshot at the moment of observation but is dynamically calculated using Time to Collision (TTC), offering a more predictive and nuanced measure of safety. Third, pedestrian safety is assessed through a dual approach: physical risk, represented by the potential for collisions between pedestrians and vehicles, and psychological safety, evaluated using proxemics theory. The latter considers metrics such as personal space—the distance within which pedestrians feel secure [19]. By leveraging objective trajectory data to measure the actual utilized feature space and quantify psychological safety, this method provides a more comprehensive and realistic assessment of pedestrian congestion and safety on mixed-use roads. Ultimately, it offers valuable insights into spatial characteristics and contributes to accident prevention strategies.

2. Related Works

2.1. Pedestrian Congestion

Research on pedestrian congestion has primarily focused on pedestrian-only roads or crosswalks, with congestion typically evaluated based on the number of pedestrians relative to the available walking area. Lower pedestrian density is commonly associated with lower congestion levels [12–15]. Similarly, Ruiz-Perez et al. [20] assessed pedestrian congestion by calculating the number of pedestrians per available walking area. They adjusted the observed pedestrian counts by incorporating data collected via Wi-Fi networks. Beyond pedestrian density-based methods, Jeon and Son [9] proposed an approach that evaluates pedestrian service levels by accounting for the loss of effective walking area when pedestrians from different directions intersect, thereby reflecting the impact of such conflicts on pedestrian space utilization.

Due to the difficulty of obtaining pedestrian trajectory data, recent studies have turned to CCTV footage to calculate pedestrian congestion or simulate pedestrian safety. Zanlungo et al. [8] used simulations to generate virtual data for assessing congestion at a narrow, crowded intersection, proposing the congestion number (CN) as a metric. The CN quantitatively evaluates dynamic pedestrian interactions under various crowd densities, speeds, and directions. Another method involves dividing CCTV footage into grid cells and measuring pedestrian movements between cells, with reduced movement indicating higher congestion [21]. Khan [7] proposed a method for identifying congested areas in large crowds by extracting pedestrian trajectories from images at a per-second interval

and calculating trajectory speed. The difference in average movement angles between trajectory points was treated as a vibration value, with higher vibrations indicating faster movement and lower vibrations indicating slower movement. These vibration values were visualized in heatmaps to identify densely populated, congested areas. In some cases, cellular base station data have been used to estimate pedestrian congestion due to the difficulty of obtaining accurate pedestrian counts or trajectories. In Seoul, South Korea, real-time population congestion levels are provided for 115 locations, categorized into four levels: "very crowded", "somewhat crowded", "normal", and "relaxed". These congestion levels are adjusted based on the current population compared to historical averages, using data collected from cellular networks [22]. Additionally, pedestrian density on backstreets has been estimated by comparing administrative district road areas with floating population data [23].

In urban environments, pedestrian congestion is predominantly measured using pedestrian density—the number of pedestrians per available walking area. Recent studies have incorporated CCTV footage to assess congestion at intersections, identify congested areas in large-scale gatherings, and estimate pedestrian congestion using cellular base station data. However, little research has been conducted on pedestrian congestion or safety that simultaneously accounts for the movement of both vehicles and pedestrians.

2.2. Proxemics

In this study, we also consider the qualitative psychological safety that pedestrians perceive in assessing pedestrian congestion and safety. This is particularly important for backstreets, where narrow spaces between buildings cause pedestrians to feel less safe when in close proximity to others. The basis for considering psychological safety can be found in the field of proxemics. Proxemics, first introduced by anthropologist Edward T. Hall, studies the relationship between human behavior, communication, and social interaction in relation to physical distance. It highlights how psychological distance can change with physical proximity, providing the foundation for spatial analysis in fields such as architecture, transportation, and urban planning [24].

Although research applying proxemics to pedestrian safety is limited, there are a few notable examples. Dosey and Meisels [25] conducted an experiment measuring participants' tension when approached by individuals of different genders and at varying distances. They found that female participants experienced tension when a male approached within an average distance of 16.2 cm, whereas tension decreased to 13.9 cm when the approaching individual was another female. This demonstrates that both the type of object moving near pedestrians and the physical proximity influence pedestrians' psychological tension. In another study, the impact of the distance between a car and passing pedestrians on the driver's psychological discomfort was measured [24]. The concept of a "comfort zone" was used to describe the minimum required space before discomfort occurred, with findings showing that discomfort was affected by the distance, speed, and number of passing pedestrians, with vehicle speed being the most influential factor.

Based on these studies, it becomes evident that psychological factors related to proxemics should be included alongside physical variables such as movement speed and vehicle–pedestrian spacing when evaluating pedestrian congestion and safety on backstreets. Thus, this study aims to develop an algorithm that incorporates pedestrian and vehicle trajectories extracted from CCTV footage, considering variables such as speed, acceleration, safety buffers, and the concept of psychological safety distance to evaluate pedestrian congestion and safety.

3. Proposed Method

3.1. Definition of Terms

The key terms used in this study are defined as follows. The formulas associated with each term will be discussed in detail in their respective sections.

- Minimum Area: The minimum area required when a pedestrian or vehicle is stationary. The Minimum Pedestrian Area is calculated by multiplying the width of the pedestrian's shoulders by their chest width while standing in an upright position, with an additional 4 cm of buffer added on each side. The Minimum Vehicle Area is determined by multiplying the average width and length of a typical Korean passenger vehicle, with an additional 2 m safety buffer added to ensure safe distancing from other vehicles or pedestrians while the vehicle is stationary (Figure 1).
- Safety Buffer: The additional area required for safety when an object is moving, based on its speed, acceleration, and distance using the TTC metric. The size of the safety buffer increases as the object moves faster and decreases as it moves slower.
- Safety Occupation Spatio-Temporal Area (categorized by pedestrians and vehicles as Pedestrian Spatio-Temporal Area (PSTA) and Vehicle Spatio-Temporal Area (VSTA)): The area occupied by an object, either stationary or in motion, over a given time period. This area is the sum of the Minimum Area and the Safety Buffer, integrated over the observed time. A larger Safety Occupation Spatio-Temporal Area indicates higher congestion on the road.
- Pedestrian Congestion: The ratio of the Safety Occupation Spatio-Temporal Area to the total spatio-temporal area of the backstreet during the observation period. A higher ratio implies that a larger portion of the road space is occupied by moving objects, indicating a higher level of congestion.
- Pedestrian Safety: A metric used to measure the safety level of the backstreet. Pedestrian safety is divided into two categories: Pedestrian-to-Pedestrian Safety (Ped-Ped Safety) and Pedestrian-to-Vehicle Safety (Ped-Vehi Safety). Pedestrian Safety is initially calculated on a per-second basis. For analysis periods longer than two seconds, the maximum value is selected from the pre-calculated per-second Pedestrian Safety values within that period to represent overall Pedestrian Safety. This value is cumulative, meaning that a higher Pedestrian Safety score corresponds to a lower actual level of safety. In other words, as the Pedestrian Safety value increases, it reflects greater potential risks in the observed area.
- Pedestrian-to-Pedestrian Safety (Ped-Ped Safety): This metric measures the safety level between pedestrians, based on the distance between them as they approach from different directions. The reference distance for this metric is 1.2 m, derived from proxemics' concept of personal space. When the distance between pedestrians is less than 1.2 m, it is assumed that psychological discomfort may arise, and this instance is counted. A higher value for Ped-Ped Safety indicates a lower level of safety.
- Pedestrian-to-Vehicle Safety (Ped-Vehi Safety): This metric measures the safety level between pedestrians and vehicles, based on the number of instances in which the safety occupation spatio-temporal areas of pedestrians and vehicles overlap. A higher value for Ped-Vehi Safety indicates a lower level of safety.

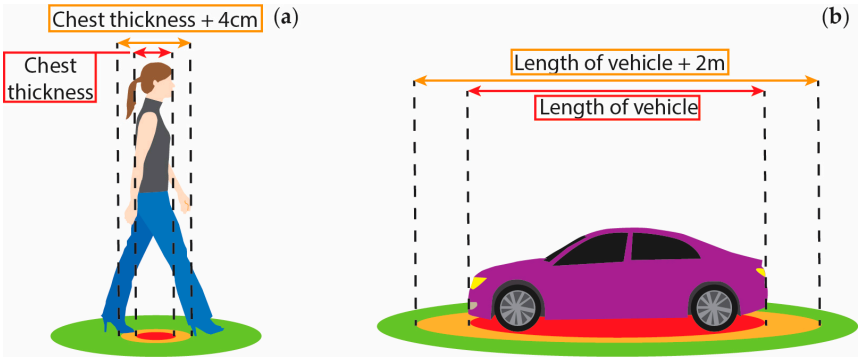


Figure 1. Concepts of minimum area and safety area. The red, orange, and green areas represent prerequisite areas where objects exist, the minimum area, and safety buffers, respectively: (**a**) pedestrian; (**b**) vehicle.

3.2. Algorithm

In this study, Pedestrian Congestion and Pedestrian Safety are calculated separately. Pedestrian Congestion is derived based on the TTC, considering the safety occupation area. Pedestrian Safety, on the other hand, is assessed by setting minimum thresholds for distances between pedestrians and between pedestrians and vehicles. The premise is that, the closer the distance between moving objects on a backstreet, the higher the risk. Pedestrian Safety is calculated based on proxemics for pedestrian-to-pedestrian interactions, while pedestrian-to-vehicle safety is measured by counting instances where the TTC-based safety occupation areas overlap.

3.2.1. TTC and Safety Buffer

Pedestrian Congestion is calculated by comparing the total area of the backstreet with the safety occupation areas of pedestrians and vehicles. The safety occupation area refers not only to static space but to dynamic spatio-temporal changes, as the space occupied by each object varies every second. This dynamic area is determined by adding a safety buffer—based on speed, acceleration, and distance to the next movement point—to the minimum required space occupied by the object. Pedestrian Congestion is the ratio of the total safety occupation area of all observed objects to the total area, observed at specific time points. The intersections of these occupation areas are used later to calculate Pedestrian Safety.

To calculate the safety buffer based on the movement information of objects, this study employs TTC. TTC was first introduced by Hayward in 1971 [26] and refers to the time remaining until a collision, assuming that the relative velocity and trajectory between two objects remain constant at a given time t [27]. TTC has been widely used to assess traffic safety [28]. The basic TTC calculation is shown in Equation (1). In this study, to account for scenarios where an object is either accelerating or not, we use Equation (2) from one of the latest studies on TTC by Wessels and Oberfeld [29].

$$\begin{aligned} \text{TTC} &= \tfrac{D(t)}{v(t)} \\ \text{D} &= \text{distance} \\ \text{v} &= \text{velocity} \\ \text{t} &= \text{time} \end{aligned} \tag{1}$$

$$\begin{aligned} \text{TTC} &= \begin{cases} \frac{-v(t)+\sqrt{2a \cdot D(t)+(v(t))^2}}{a}, & a \neq 0 \\ \frac{D(t)}{v(t)}, & a = 0 \end{cases} \\ \text{D} &= \text{distance} \\ \text{v} &= \text{velocity} \\ \text{t} &= \text{time} \\ \text{a} &= \text{acceleration} \end{aligned} \tag{2}$$

The original use of TTC calculates the expected time to collision between two distinct objects based on their speed, acceleration, and relative distance. However, in this study, TTC is used not to measure collision time between different objects, but to estimate the time it takes for an object to reach its next position 1 s later from its current position. This method allows us to calculate not only the minimum required space based on current speed and acceleration but also the necessary safety buffer to prevent collisions with other moving objects.

The data collection interval in this study is set to 1 s. Since the data are collected at 1 s intervals, the TTC used as the baseline for collision prediction is also set to 1 s. Using the object's current attributes, such as speed and acceleration, we calculate the expected time to reach the next point 1 s ahead, which allows us to determine the safety buffer beyond the minimum required area for movement. In cases where TTC is calculated to be less than 1 s, the object is moving quickly, indicating that a larger safety buffer is required. If TTC is greater than 1 s, the object is moving more slowly, meaning a smaller safety buffer is sufficient.

Additionally, there are cases wherein TTC may be calculated as 0 or approaches zero, as well as cases where it is infinite. These indicate that the object's current and future positions overlap, which, for two separate objects, would signify a collision. However, in this study, since we are calculating the trajectory of a single object at both its current and next positions, overlapping positions indicate that the object is stationary. In such cases, only the minimum required area for the stationary object is considered, without adding a safety buffer (Algorithm 1).

Algorithm 1 TTC and Buffer Area Calculation

Function TTC (data, trajec_id, type_code)
$D \leftarrow$ distance between now and next point of data
$v \leftarrow$ speed of data
$a \leftarrow$ acceleration of data
type_code $\leftarrow$ type_code
if $v == 0$ **then**
$ttc \leftarrow \infty$
elif $a == 0$ **then**
$ttc \leftarrow \frac{D}{v}$ **if** $v \neq 0$ **else** ∞
else
$discriminant \leftarrow (2 \cdot a \cdot D) + v^2$
$ttc \leftarrow \frac{-v+\sqrt{discriminant}}{a}$ **if** $discriminant \geq 0$ **else** ∞
$ttc \leftarrow 0$ **if** $ttc == -0.0$ **else** ttc
return ttc

Function BUFFER_AREA (ttc, object_length, object_width)
► object_length, object_width are include safety length already
width $\leftarrow$ object_width
length $\leftarrow$ object_length
minimum_area $\leftarrow$ width·length
if $ttc == \infty$ **then** ► Already considered as collided
total_v $\leftarrow$ minimum_area
elif $ttc < 0.1$ **then** ► Already considered as collided
total_v $\leftarrow$ minimum_area
else
safety_area $\leftarrow \left(\frac{1}{ttc}\right) \cdot$ minimum_area
PSTA or VSTA $\leftarrow$ safety_area + minimum_area
return PSTA or VSTA

Equations (3) and (4) are used to calculate the PSTA and VSTA. These areas are calculated on a per-second basis, and by integrating the per-second safety occupation area over the observation time t, the spatio-temporal area for the observed object over the observation time t is determined. Pedestrians and vehicles each have distinct minimum required areas, denoted by P and V, respectively.

$$\begin{gathered} P_{STA} = \int_0^T D(t)dt \\ D(t) = P + B(ttc) \\ P = \textit{minimum pedestrian area} = (4\text{ cm} + \textit{length} + 4\text{ cm}) \times (4\text{ cm} + \textit{width} + 4\text{ cm}) \\ B(ttc) = \textit{safety buffer} = \frac{1}{TTC} \times P \\ \textit{length} = \textit{shoulder length} = 0.417\text{ m} \\ \textit{width} = \textit{chest thickness} = 0.233\text{ m} \end{gathered} \tag{3}$$

$$\begin{gathered} V_{STA} = \int_0^T D(t)dt \\ D(t) = V + B(ttc) \\ V = minimum\ vehicle\ area = (length + 2\ \mathrm{m}) \times (width + 2\ \mathrm{m}) \\ B(ttc) = safety\ buffer = \frac{1}{TTC} \times V \\ length = vehicle\ length = 4.7\ \mathrm{m} \\ width = vehicle\ width = 1.7\ \mathrm{m} \end{gathered} \tag{4}$$

The minimum required area for pedestrian (P) is calculated using a median shoulder length of 0.417 m and a median chest width of 0.233 m based on the anthropometric data of Koreans surveyed in 2021 [30]. An additional buffer of 4 cm is added to each side to account for lateral sway during walking [16,31]. For vehicles, the minimum required area (V) is determined using the standard dimensions of a passenger car in Korea, where the width and length are 1.7 m and 4.7 m, respectively, as specified by the Korean Ministry of Land, Infrastructure, and Transport. Additionally, a safety buffer of 2 m is added to both the width and length, resulting in final dimensions of 3.7 m and 6.7 m. The 2 m buffer corresponds to the minimum safe stopping distance typically maintained between a vehicle and a crosswalk on a road when the vehicle is stationary.

The Safety Occupation Spatio-Temporal Areas (PSTA and VSTA) vary depending on how the TTC changes relative to the 1 s threshold. According to Equation (2), if the acceleration is zero, the TTC and safety buffer are determined by the instantaneous speed of the trajectory point and the distance to the next point. The safety buffer added to the basic minimum required area depends on whether the acceleration is zero, positive, or negative.

3.2.2. Pedestrian Congestion

The Pedestrian Congestion level on the backstreets is calculated as the ratio of the combined spatio-temporal areas occupied by all moving objects passing through the observed backstreets during the observation period to the total spatio-temporal area of the road as shown in Equation (5).

$$\begin{gathered} Pedestrian\ Congestion(PC) = \frac{P_{STA} + V_{STA}}{STA} \\ STA = road\ length \times road\ width \times time\left(\mathrm{m}^2 \cdot \mathrm{s}\right) \end{gathered} \tag{5}$$

The Pedestrian Congestion index is derived as a ratio between 0 and 1, where values closer to 0 indicate low congestion, while values closer to 1 suggest high congestion. If the ratio exceeds 1, it indicates that the entire road area has been utilized, and the value is adjusted to 1. To calculate the total safety occupation area of all objects during the observation period, the safety buffers of each object are generated and aggregated at 1 s intervals. This aggregated buffer is then integrated over an hour to compute the pedestrian congestion level.

3.2.3. Pedestrian Safety

(1) Ped-Ped Safety

Pedestrian-to-pedestrian (Ped-Ped) safety is assessed by identifying potential threats when one pedestrian's personal space, as defined by proxemics, is encroached upon by another pedestrian (Table 1). This is quantified by counting the number of opposing-direction trajectories that come within 1.2 m of each trajectory point. The threshold of 1.2 m is derived from the four spatial zones outlined in proxemics [19]. Distances exceeding 1.2 m fall within the social or public space, which is more appropriate for interactions in environments where encounters with strangers are common and unremarkable. In contrast, personal space—defined as the area within 1.2 m—is generally reserved for interactions with familiar individuals. As noted in [32], objective measures of spatial boundaries, such as personal space, have a stronger correlation with human behavior in built environments than subjective perceptions. These spatial boundaries significantly influence walking patterns and perceptions of safety. In this context, a breach of personal space by unfamiliar

individuals can cause discomfort, especially in shared public spaces where interactions are often involuntary. Only interactions between pedestrians moving in opposite directions are analyzed, based on walking direction (0: same direction, 1: opposite direction). This approach assumes that pedestrians traveling in the same direction are more likely to be companions, while those moving in opposite directions are more likely to evoke feelings of discomfort or unfamiliarity when invading each other's personal space.

Table 1. Definition of the four levels of proxemics distances [19].

Level	Distance	Psychological Meaning
Intimate Space	~45 cm	The distance in close relationships such as those with a partner or family
Personal Space	45 cm~1.2 m	The distance within arm's reach, allowing friends and acquaintances to gauge each other's emotions
Social Space	1.2 m~3.6 m	The distance for business and formal interactions
Public Space	3.6 m~7.6 m	A distance that is easy to retreat from in case of threat, where voices are raised and non-verbal communication becomes more active

(2) Ped-Vehi Safety

Ped-Vehi Safety is calculated by counting the number of instances where the TTC-based safety occupation areas of pedestrians and vehicles overlap. The direction of movement for both pedestrians and vehicles is not considered in this calculation, as the risk of collision increases regardless of direction when pedestrians and vehicles are in close physical proximity. Ped-Vehi Safety is determined by aggregating the intersections of PSTA and VSTA, with higher counts indicating a greater number of potential collision points between pedestrians and vehicles. Ped-Vehi Safety and Pedestrian Congestion are calculated simultaneously to enhance computational efficiency. By using spatial join techniques, we reduce unnecessary repeated calculations and increase the computational speed by processing both algorithms in parallel.

Algorithm 2 presents the pseudocode for the algorithm that simultaneously calculates Pedestrian Congestion and Ped-Vehi Safety. It begins by generating geometric buffers for PSTA and VSTA based on TTC. The TTC-based geometric buffers are created by calculating the buffer radius as $\sqrt{area/\pi}$ using the PSTA and VSTA areas for pedestrians and vehicles, respectively, and applying this radius to generate geometric buffers around each point. Then, it joins these buffers to compute both the intersections and unions. To identify overlapping areas between pedestrian and vehicle buffers, a spatial join operation is performed using the sjoin function from GeoPandas, with the predicate intersects to locate intersecting regions. Additionally, to calculate the total safety occupation area, the unary union function from the Shapely library is applied to unify pedestrian and vehicle buffers, avoiding overlap duplication when computing the union.

1. Both pedestrians and vehicles are present: Ped-Vehi Safety is calculated as the intersection of PSTA and VSTA, while Pedestrian Congestion is calculated with the sum of the PSTA and VSTA areas.
2. Only pedestrians are present: Ped-Vehi Safety returns 0, and Pedestrian Congestion is calculated with the sum of the PSTA areas.
3. Only vehicles are present: Ped-Vehi Safety returns 0, and Pedestrian Congestion is calculated with the sum of the VSTA areas.
4. No objects are present: Both Ped-Vehi Safety and Pedestrian Congestion return 0.

This structure ensures that both safety and congestion metrics are efficiently computed for varying conditions, accounting for the interactions between pedestrians and vehicles on shared road spaces.

Algorithm 2 Calculating Buffered Geometry and Intersections

```
Function CALCULATE_TTCBUFFER_GEOMETRY(df)
    Create a GeoDataFrame from the DataFrame and apply the buffer
    Convert the coordinate reference system to "EPSG:5179" to calculate buffer as a meter
    Calculate the buffer radius from the buffer area using the formula: sqrt(area/π)
    Apply the buffer to the geometry using the calculated radius
    Set the buffered geometry as the default geometry column
    Create a spatial index for the GeoDataFrame
    return geo_pd

Function CALCULATE_INTERSECTION(pedestrian, vehicles)
    Check if the pedestrian DataFrame is not composed only of NaN values
  if pedestrian DataFrame is not NaN then
        Check if the vehicles DataFrame is not composed only of NaN values
    if vehicles DataFrame is not NaN then ► Both pedestrians and vehicles exist
            Calculate the buffered geometry for pedestrians
            Calculate the buffered geometry for vehicles
            Perform a spatial join to find intersecting objects using the predicate "intersects"
            Combine all pedestrian and vehicle buffers and calculate the union of these buffers
            Calculate the area of the union
            Return intersections.shape[0], union_area
      else ► Only pedestrians exist
            Calculate the buffered geometry for pedestrians
            Calculate the union of all pedestrian buffers
            Calculate the area of the union
            Return 0, union_area
      end if
else
        Check if the vehicles DataFrame is not composed only of NaN values
    if vehicles DataFrame is not NaN ► Only vehicles exist
        Calculate the buffered geometry for vehicles
        Calculate the union of all vehicle buffers
        Calculate the area of the union
        return 0, union_area
    else ► Neither pedestrians nor vehicles exist
        return 0, 0
    end if
end if
```

4. Experiments

4.1. Experimental Setup

4.1.1. Workflow

To verify the suitability of the proposed algorithm, real-world data were used to calculate Pedestrian Congestion and Pedestrian Safety. The overall workflow is shown in Figure 2. After preprocessing pedestrian and vehicle trajectory data collected from CCTV, the Safety Buffer for pedestrians and vehicles was calculated using TTC, and this was used to compute Pedestrian Congestion and Ped-Vehi Safety. Ped-Ped Safety was measured by calculating the distance between pedestrians moving in opposite directions to assess situations wherein psychological discomfort could arise. After calculating both Pedestrian Congestion and Pedestrian Safety, a paired *t*-test and a K-S (Kolmogorov–Smirnov) test were conducted to examine whether there were significant differences between the results of the proposed algorithm and existing pedestrian density calculations. A Bland–Altman plot was used to test whether the algorithm could serve as an alternative to traditional pedestrian density measures. Finally, the data buffers were visualized as snapshots to compare the Pedestrian Congestion results from the algorithm with the pedestrian density from Korea Highway Capacity Manual (KHCM). This comparison was intended to assess how well the new algorithm reflects real-world pedestrian congestion compared to existing standards.

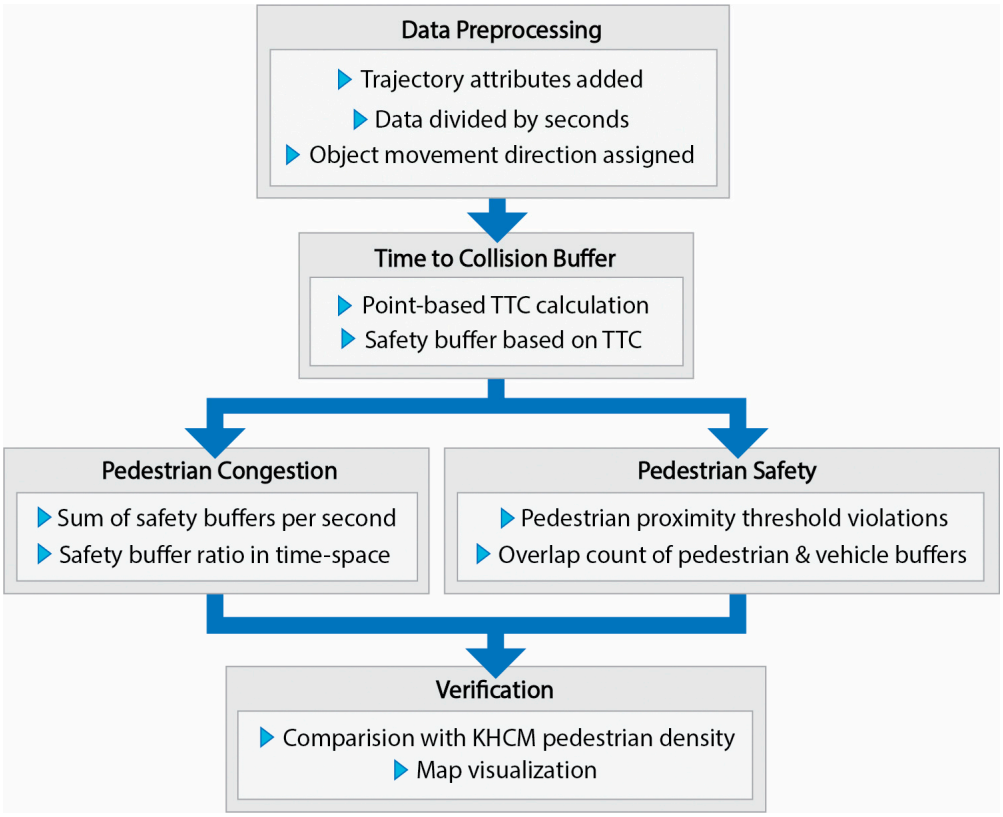


Figure 2. Workflow of the experiment.

4.1.2. Data

The data used in this study consist of pedestrian and vehicle trajectory points extracted from 12 CCTV cameras installed along the backstreets of the Indeokwon area in Anyang, South Korea. Figure 3 shows the CCTV locations on a map. The observation period spans from 12:00 p.m. on 6 December 2023, to 4:00 p.m. on 20 December 2023, with data collected at 1 s intervals. The neighborhood characteristics of the backstreets captured by each CCTV camera are detailed in Table 2.



Figure 3. The location of CCTVs.

Table 2. Neighborhood characteristics by CCTV.

CCTV	Neighborhood Characteristics
V0000, V0001, V0002, V0003, V0005, V0007	A bustling commercial area consisting of restaurants and karaoke rooms surrounding a park
V0008, V0010, V0011	A residential complex with the first floor consisting of commercial shops
V0016, V0018, V0019	An intersection composed of a dining alley, karaoke rooms, massage shops, and franchise restaurants adjacent to a cluster of medical facilities

The data used in this study comprise a total of 3,044,706 trajectories collected from 12 CCTV cameras over a 15-day period, with 98,647,066 trajectory points. The collected objects include both pedestrians and vehicles, and the data were captured at the point level for each object. The data were preprocessed by grouping points by object ID to generate trajectories, as shown in Figure 4. In addition to the unique ID, object type, latitude and longitude coordinates, and timestamp, mobility-related attributes such as speed, acceleration, heading angle, turning angle, and distance to the previous trajectory point were added for each point. Moreover, the trajectory's direction—whether the pedestrian was moving forward or in the opposite direction—was determined by comparing the heading angle of the trajectory point with the road alignment and added as an attribute. Using Python libraries, including GeoPandas and MovingPandas, additional attributes were calculated and added, as shown in Table 3, to facilitate the calculation of Pedestrian Congestion and Pedestrian Safety.

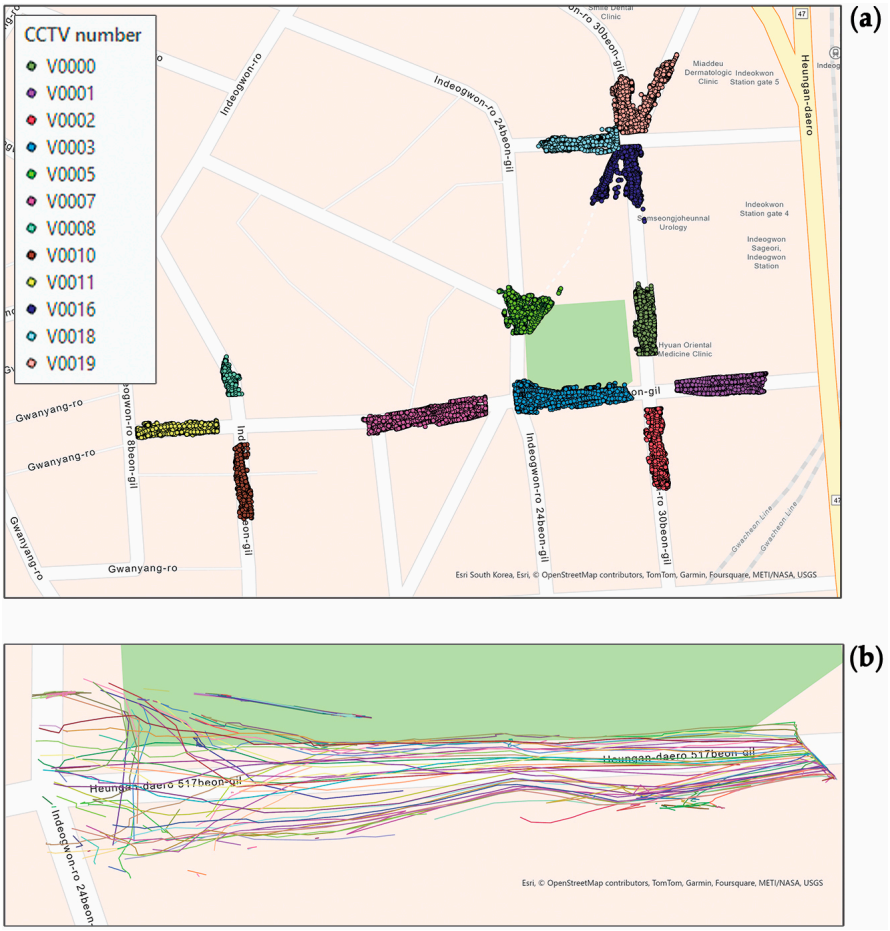


Figure 4. A sample of the raw data: (**a**) data points from CCTV between 13:00 and 14:00 on December 6th; (**b**) trajectories for CCTV V0003, where points are connected by object ID.

Table 3. Attributes of data.

	Name	Attribute	Unit
Original Attributes	id	Unique Trajectory ID	Number
	type_code	Object Type	1 (Pedestrian)/2 (Car)
	X	Longitude	Number
	Y	Latitude	Number
	t	Collection Date and Time	YY-MM-DD hh:mm:ss
Added Attributes	acceleration *	Acceleration	m/s^2
	angular_difference *	Degree of Object Direction Change	0~360°
	direction *	Object Travel Direction	0~360°
	speed *	Speed	m/s
	distance	Distance Between Current and Subsequent Object Points	m
	bi-direction	bi-direction of feature	0: Forward/1: Reverse

* Calculated using the current and previous points.

4.2. Experimental Results

4.2.1. Pedestrian Congestion

The hourly Pedestrian Congestion data for December 8 and 9 are presented in Figure 5. Pedestrian Congestion is represented as a ratio between 0 and 1, with values closer to 1 indicating higher congestion. The V0019 area exhibited the highest Pedestrian Congestion across all observed dates, followed by the V0003 area. The V0001 area had the lowest Pedestrian Congestion. During the 15-day observation period, congestion was generally low between 2:00 a.m. and 7:00 a.m., while higher congestion was observed from 2:00 p.m. to the evening hours. The results also demonstrate significant variations in Pedestrian Congestion across different CCTV-monitored areas, which is likely attributable to the differing characteristics of the surrounding neighborhoods and the varying volume of people and vehicles visiting each backstreet. These findings highlight the importance of considering localized factors when assessing Pedestrian Congestion on backstreets.

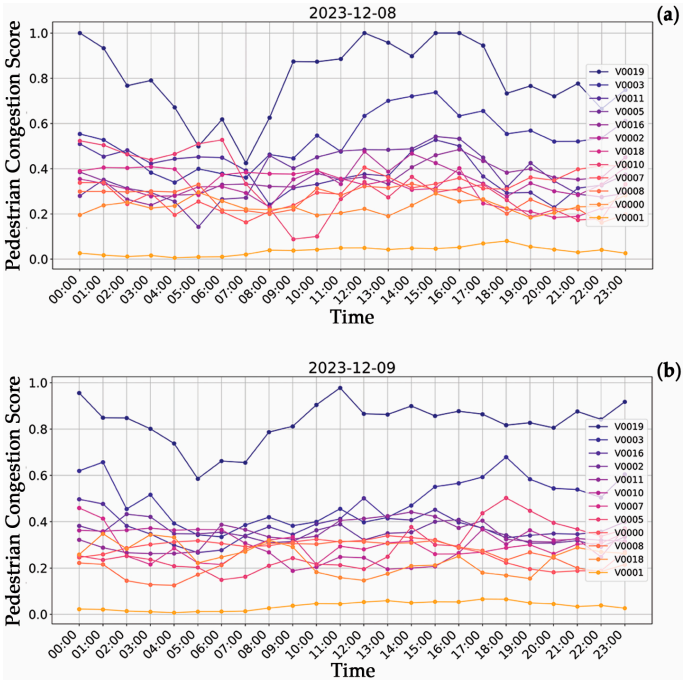


Figure 5. Hourly Pedestrian Congestion plots: (**a**) December 8th; (**b**) December 9th.

Figure 6 presents heatmaps of Pedestrian Congestion by time of day and CCTV location for December 7 and 16. Since December 7 was a Thursday and December 16 was a Saturday, and differences in Pedestrian Congestion patterns can be observed. These differences can be interpreted in connection with the surrounding neighborhoods. For example, in the V0003 area, which is located near a cluster of restaurants, pedestrian congestion remained consistently high on both weekdays and weekends. However, it reached its peak on Saturday between 5:00 p.m. and 6:00 p.m., likely due to increased foot traffic around dining hours. In contrast, the V0010 area exhibited marked differences between weekdays and weekends. This road is located in a residential area, suggesting that the variation in pedestrian and vehicle traffic may be due to residents traveling elsewhere or staying home during weekends, resulting in lower road traffic compared to weekdays. These observations underscore the influence of local land use and infrastructure on pedestrian congestion patterns, particularly when comparing weekdays and weekends.

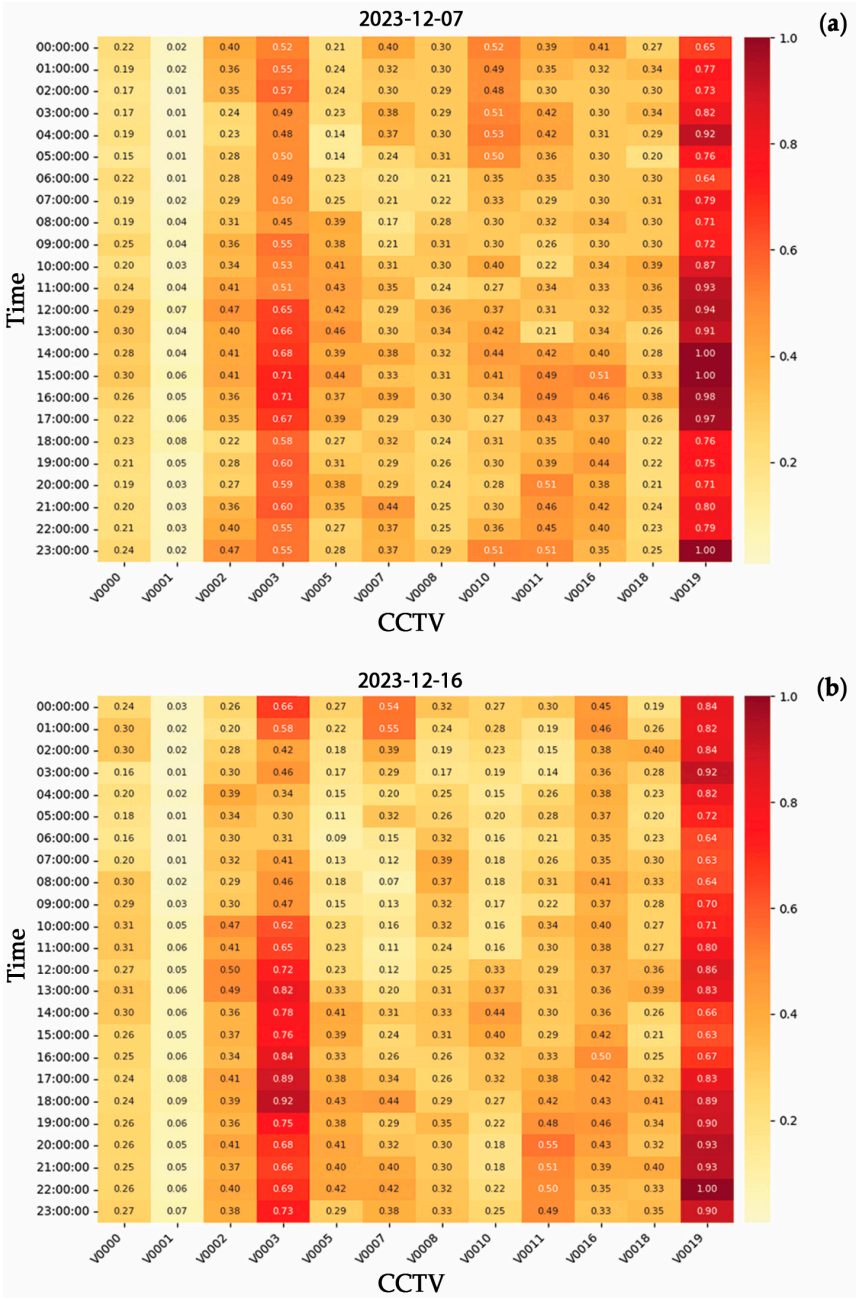


Figure 6. Heatmaps of Pedestrian Congestion: (**a**) 7th of December; (**b**) 16th of December.

4.2.2. Pedestrian Safety

The visualization of Pedestrian Safety for the V0001 and V0019 areas over 14 days is shown in Figure 7. Pedestrian Safety was calculated by distinguishing between Ped-Ped Safety and Ped-Vehi Safety, with the maximum value within each analysis interval t used for the final safety score. This approach focuses on capturing the most dangerous situations. Figure 7 illustrates the safety scores on an hourly basis, where higher values indicate greater danger.

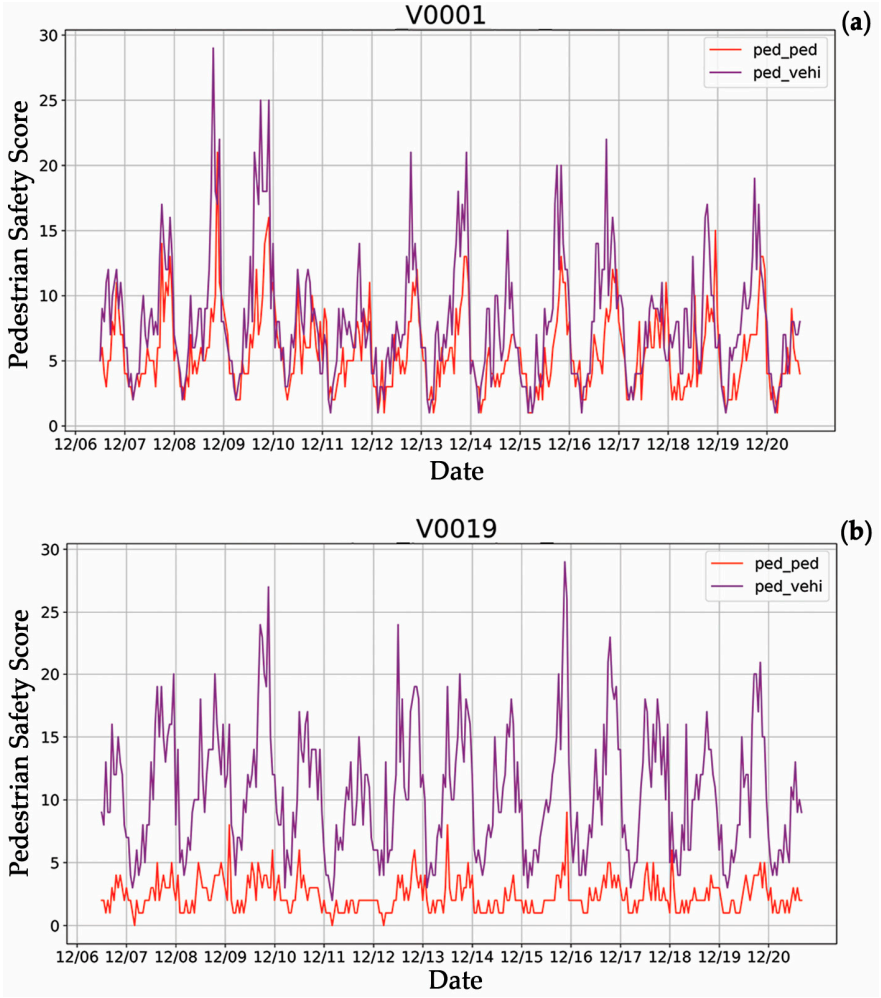


Figure 7. Pedestrian Safety plots: (**a**) CCTV V0001; (**b**) CCTV V0019.

The analysis revealed that the likelihood of collisions increased in the evening, particularly when pedestrian and vehicle activity was higher. A notable finding is that, for almost all CCTV-monitored areas, the likelihood of pedestrian-to-vehicle collisions was significantly higher than pedestrian-to-pedestrian collisions. This suggests that, on these backstreets, the risk of collisions between pedestrians and vehicles is greater than that between pedestrians themselves. Furthermore, since Ped-Vehi Safety is based on TTC-derived safety occupation areas, higher scores reflect moments where the number of nearby vehicles or their speeds posed significant danger to pedestrians.

Pedestrian Safety also showed variation depending on the day of the week. On weekends, particularly from Friday to Sunday (8th–10th and 15th–17th), most CCTV areas reported higher safety scores, indicating lower safety. This can be interpreted as an increase in pedestrian and vehicle traffic during weekends, resulting in a higher risk of collisions. Furthermore, the patterns of Ped-Ped Safety and Ped-Vehi Safety varied by CCTV area. For example, in the V0001 area, the patterns of Ped-Ped Safety and Ped-Vehi Safety were

similar, whereas in the V0019 area, Ped-Ped Safety was relatively safe, but Ped-Vehi Safety had high scores, indicating greater risk. This discrepancy highlights the varying dynamics of pedestrian safety depending on the local context of each backstreet.

4.3. Algorithm Validation

4.3.1. Evaluation Metrics

To validate the suitability of the proposed algorithm, two evaluation methods were employed. First, we assessed whether there was a statistically significant difference between the Pedestrian Congestion results calculated using our algorithm and the Pedestrian Density metrics provided by the KHCM. Second, we performed a Bland–Altman analysis to visually confirm whether the proposed algorithm achieves a similar level of accuracy in data measurement compared to existing methods.

For statistical validation, we conducted paired-sample *t*-tests and K-S tests on the hourly Pedestrian Congestion score generated by our algorithm and the Pedestrian Density score calculated by Equation (6) from the KHCM [33]. The KHCM's Pedestrian Density metric calculates the average number of pedestrians relative to the total road area, and the corresponding levels of pedestrian service are shown in Table 4. Level A represents the highest service level, indicating a comfortable walking environment, while level F indicates congestion. The paired-sample *t*-test shown in Equation (7) was used to statistically evaluate whether there was a significant difference in the mean values between the results from the proposed algorithm and the traditional method [34]. In this equation, T is the *t*-test statistic, $\overline{D}$ is the mean difference between the two datasets, s_D is the standard deviation of the differences, and n is the sample size. A smaller *p*-value supports the hypothesis that there is a significant difference between the two methods.

Table 4. Pedestrian service level of KHCM [34].

Level	Density (People/m^2)
A	≤0.3
B	≤0.5
C	≤0.7
D	≤1.1
E	≤2.6
F	>2.6

The K-S test is a non-parametric test that compares two cumulative distribution functions to determine whether they come from the same distribution [35]. In this study, we employed the K-S two-sample test, as shown in Equation (8), to compare the distributions of the two samples. In the equation, D is the K-S test statistic, sup_x represents the maximum difference for x, and $F_1(x)$ and $F_2(x)$ are the empirical cumulative distribution functions for the two samples. A smaller *p*-value supports the hypothesis that the distributions of the two datasets are different. This dual approach of statistical and visual validation provides a comprehensive assessment of whether the proposed algorithm can serve as a reliable alternative to conventional pedestrian density metrics.

$$Average\ Pedestrian\ Density = \frac{\frac{1}{T}\sum_{t=1}^{T} pedestrian_t}{Road\ Area} \tag{6}$$

$$T = \frac{\overline{D}}{s_D/\sqrt{n}} \tag{7}$$

$$D = sup_x|F_1(x) - F_2(x)| \tag{8}$$

The Bland–Altman analysis is used to examine the agreement between two methods, providing a visual assessment of whether the proposed algorithm measures data with similar accuracy to traditional methods [36]. This analysis is commonly used in clinical

settings to evaluate the consistency between a new method and an existing one, where high consistency indicates that the new method can serve as a replacement for the traditional approach [37]. A Bland–Altman plot interprets the difference between the two methods by analyzing the mean difference, the distribution of the data, and the limits of agreement. The mean difference represents the bias between the two datasets, shown as the central line in the plot. A bias close to zero indicates no significant difference between the two methods. The distribution of the data is usually represented by a scatter plot, and a concentration of points near the center suggests no systematic differences between the two methods. The 95% limits of agreement are calculated as the mean difference plus and minus 1.96 times the standard deviation, as represented in Equation (9). Narrower limits of agreement indicate that the two methods are closely aligned. Through this methodology, the algorithm can be shown to produce statistically distinct results from traditional Pedestrian Density measurement methods, while also demonstrating sufficient agreement to be considered a clinically acceptable alternative. Through this methodology, the algorithm can be shown to produce statistically distinct results from traditional Pedestrian Density measurement methods, while also demonstrating sufficient agreement to be considered a clinically acceptable alternative.

$$\begin{aligned} &Upper\ Limit\ of\ Agreement \\ &\quad = mean\ difference + 1.96 \times standard\ deviatioin \\ &Lower\ Limit\ of\ Agreement \\ &\quad = mean\ difference - 1.96 \times standard\ deviation \end{aligned} \tag{9}$$

4.3.2. Statistics Validation

The results of the *t*-test and K-S test comparing Pedestrian Congestion with KHCM Pedestrian Density are shown in Table 5. Both statistical tests show that the *p*-values for all CCTV locations are significantly smaller than the threshold of 0.05, indicating statistical significance. The *t*-test results demonstrate that the mean difference between Pedestrian Congestion and Pedestrian Density is statistically significant, proving that Pedestrian Congestion, as calculated by the proposed algorithm, represents a distinct measurement method from traditional Pedestrian Density. Similarly, the K-S test results indicate that the distributions of the two metrics differ, suggesting that the two methods analyze data from different perspectives. This can be interpreted as evidence that the proposed algorithm measures the pedestrian environment from a new angle. These findings confirm that the Pedestrian Congestion calculated in this study and the Pedestrian Density from KHCM exhibit statistically significant differences. Thus, the proposed algorithm provides a novel measurement approach distinct from the traditional distribution of Pedestrian Density.

Table 5. Paired sample *t*-test and two-sample K-S test between Pedestrian Congestion and Pedestrian Density.

CCTV	t-Stats	*p*-Value	K-S Stats	*p*-Value
V0000	98.8691	<0.0001	1.0000	<0.0001
V0001	30.8659	<0.0001	0.8768	<0.0001
V0002	67.1417	<0.0001	1.0000	<0.0001
V0003	68.5373	<0.0001	1.0000	<0.0001
V0005	48.0672	<0.0001	0.9941	<0.0001
V0007	56.5825	<0.0001	1.0000	<0.0001
V0008	120.1083	<0.0001	1.0000	<0.0001
V0010	46.2439	<0.0001	0.9971	<0.0001
V0011	67.8659	<0.0001	1.0000	<0.0001
V0016	63.0891	<0.0001	1.0000	<0.0001
V0018	64.2722	<0.0001	1.0000	<0.0001
V0019	115.9746	<0.0001	1.0000	<0.0001

4.3.3. Bland–Altman Analysis Validation

The Bland–Altman plot comparing the Pedestrian Congestion calculated by the proposed algorithm and the Pedestrian Density from the KHCM is shown in Figure 8. The figure presents the Bland–Altman plots for the V0003 and V0007 areas. In both scatter plots, the data points exhibit a linear dispersion pattern. As the difference between the two datasets increases, the mean of the two measurements also increases. This suggests that, as Pedestrian Congestion increases, the difference between Pedestrian Congestion and Pedestrian Density becomes more pronounced. This increasing divergence as the mean value grows is important evidence that the proposed algorithm provides information distinct from traditional pedestrian density measurements. Specifically, it indicates that our algorithm, by including interactions with vehicles, offers a more comprehensive assessment of congestion and safety in real-world settings. The larger Pedestrian Congestion scores are likely driven by the additional safety occupation areas of vehicles and pedestrians, which are accounted for in the Pedestrian Congestion calculation but not in the Pedestrian Density metric. This indicates that the divergence between the two measurement methods is largely influenced by the TTC-based safety occupation areas and the presence of vehicles, which are factors not considered in traditional Pedestrian Density measurements.

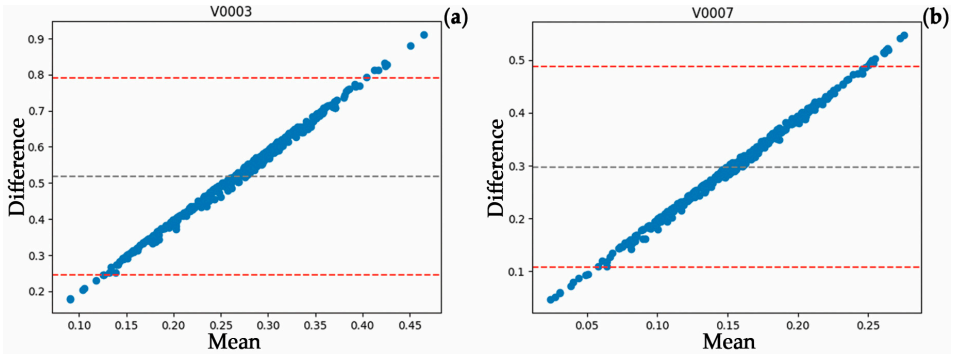


Figure 8. Bland–Altman plots for Pedestrian Congestion and KHCM Pedestrian Density. The gray line denotes the mean of the two datasets, and the red lines denote the 5% and 95% limits of agreement: (**a**) V0003; (**b**) V0007.

Additionally, since the majority of the data points fall within the 95% limits of agreement, we can conclude that the Pedestrian Congestion and Pedestrian Density metrics are in general agreement in terms of their interpretation of congestion levels. The absence of substantial bias between the two methods further indicates that the proposed algorithm produces results comparable to those of traditional Pedestrian Density measurements. The statistical analysis and data consistency validation demonstrate that the proposed Pedestrian Congestion algorithm is a reliable and clinically acceptable alternative to existing methods for measuring pedestrian density.

4.3.4. Compared Visualization

To provide a more detailed comparison between Pedestrian Congestion and Pedestrian Density, the hourly Pedestrian Congestion results from the proposed algorithm and the Pedestrian Density from the KHCM are shown in Figure 9. The red line, representing Pedestrian Congestion, exhibited more dynamic changes over time and date compared to the purple line, which denotes Pedestrian Density. In both backstreets monitored by the two CCTVs, the Pedestrian Density suggests that these areas consistently experience low pedestrian volumes, indicating a generally comfortable walking environment. However, according to the Pedestrian Congestion results from this study, both locations showed significant congestion during the afternoon hours on all observed dates. This highlights the proposed algorithm's ability to capture dynamic variations in congestion, especially in

scenarios where traditional Pedestrian Density metrics may fail to account for factors such as vehicle presence and varying pedestrian flow patterns.

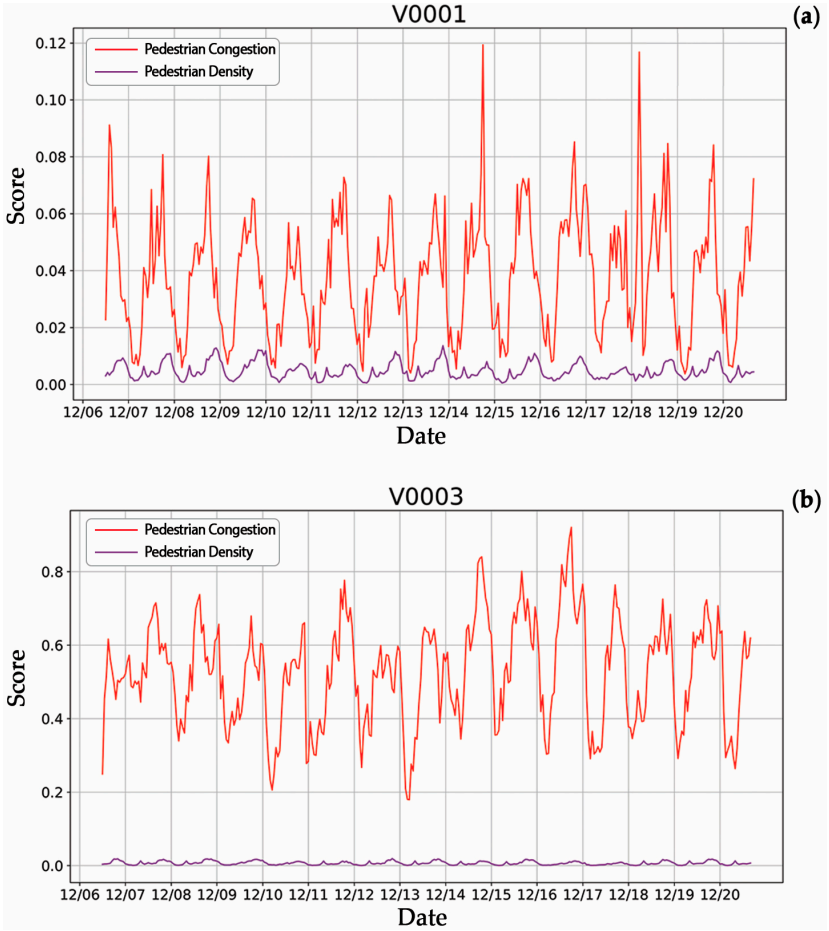


Figure 9. Comparison between Pedestrian Congestion and KHCM Pedestrian Density score for (**a**) V0001 and (**b**) V0003.

The visualization of the Safety Occupation Spatio-Temporal Area, along with the calculated Pedestrian Congestion, Pedestrian Safety, and Pedestrian Density metrics, is shown in Figure 10. This figure represents the V0001 area at 15:58:28 on 20 December 2023. Despite the relatively low number of vehicles, Pedestrian Congestion was found to be high in this area due to the large VSTA buffers of two vehicles, represented by the green circles. The speed of the vehicle corresponding to the largest circle is 1.676368 m/s, and the second largest vehicle's speed is 4.352353 m/s, which convert to 6.03 km/h and 15.67 km/h, respectively. On this narrow backstreet, the movement of these two vehicles reduced the available space for both pedestrians and other vehicles, contributing to the high Pedestrian Congestion. Ped-Vehi Safety was recorded as four instances, and it was observed that the PSTA of most pedestrians overlapped with the VSTA of the moving vehicles, except for one pedestrian. The Pedestrian Density from the KHCM for this area is 0.005, with a pedestrian level of service rated as Level A, indicating a smooth flow. However, based on the analysis using this study's algorithm, considering the relationship between moving vehicles and nearby pedestrians, along with the Pedestrian Congestion and Pedestrian Safety values, it can be concluded that, at the moment of observation, the V0001 road was congested, and there was a potential risk of pedestrian–vehicle collisions. This comparison underscores the importance of considering vehicle presence and movement when evaluating Pedestrian Congestion and Safety, especially in mixed-use environments such as narrow backstreets.

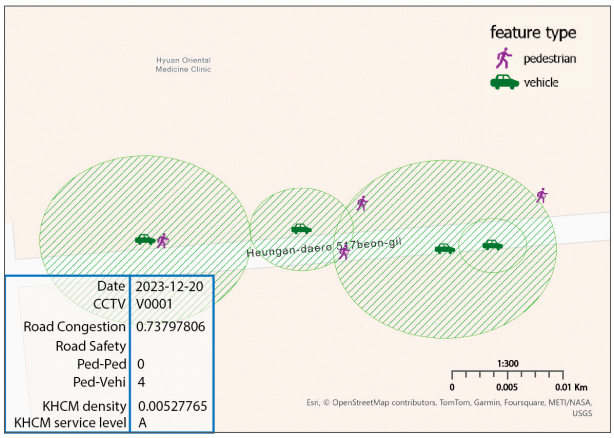


Figure 10. Visualization of P_{STA} and V_{STA} for V0001 on 20 December 2023. The green and purple circle represent V_{STA} and P_{STA} buffer, respectively.

5. Conclusions

Unlike major roads or arterials where sidewalks and roadways are clearly separated, alleyways present unique challenges for pedestrian safety and congestion due to parked vehicles and moving traffic that often reduce usable space. These factors pose significant risks to pedestrian safety, making it crucial to account for both pedestrians and vehicles when measuring Pedestrian Congestion and Safety on alleyways. Moreover, since vehicle movement and parking continuously change in these spaces, it is essential to incorporate such dynamic conditions into the calculation of pedestrian congestion and safety. In this context, the aim of this study was to develop an algorithm for measuring Pedestrian Congestion and Pedestrian Safety on alleyways.

Pedestrian Congestion was calculated based on TTC using safety occupation areas, while Pedestrian Safety was determined by setting minimum thresholds for pedestrian-to-pedestrian and pedestrian-to-vehicle distances and recording instances wherein safety buffers overlapped. The threshold for Ped-Ped Safety was established using the concept of proxemics, while Ped-Vehi Safety was measured by aggregating TTC-based safety occupation areas. The proposed algorithm was applied to real-world data, visualized, and statistically validated. The experimental results show variations in Pedestrian Congestion and Safety based on observation time and location, enabling the measurement of congestion and risk according to the spatio-temporal characteristics of each alleyway. Notably, the incorporation of both pedestrian and vehicle movement allowed for a more refined measurement of alleyway congestion compared to traditional Pedestrian Density metrics that consider only pedestrian movement.

The contributions and distinctiveness of this study are as follows. First, by measuring the real-time changes in the occupation areas of pedestrians and vehicles, the algorithm provided a more precise assessment of real-world congestion compared to existing methods. Second, unlike previous studies that focused solely on pedestrians, this study considered both pedestrians and vehicles when measuring Pedestrian Congestion and Pedestrian Safety in areas without clear separation between sidewalks and roadways. Third, the separation of Pedestrian Safety from Pedestrian Congestion allowed the algorithm to measure not only the potential for physical collisions between objects but also the psychological discomfort felt by pedestrians, which is another distinguishing feature of this study.

The results of this study provide specific congestion and safety values for alleyways at given moments in time. Narrowly, these results can contribute to basic information about road conditions, while broadly, they hold significance as reference data for public services and policy decisions aimed at improving road safety and flow. For example, if a particular section of an alleyway is found to be congested at specific times, policies could be implemented to limit vehicle access during those times to facilitate smoother pedestrian flow. Similarly, if certain alleyways are consistently identified as unsafe, services such as

reduced vehicle speed limits or safety patrols could be introduced to enhance pedestrian security in those areas. Furthermore, the proxemics-based psychological measures proposed in this study could extend beyond identifying congestion and safety zones to extracting extreme congestion areas. This capability could aid in recommending avoidance routes, thus supporting pedestrian decision-making and improving overall mobility efficiency. Future studies could integrate behavioral data and traffic psychology principles to enhance psychological safety measures and optimize pedestrian and vehicle flow in real time.

While the Pedestrian Safety measure in this study considers the psychological safety of pedestrians based on the distance between approaching pedestrians, there are limitations. For instance, the algorithm does not account for cases wherein approaching pedestrians are companions or acquaintances, which would mitigate the sense of psychological discomfort. This limitation arises from the difficulty of extracting such information from the available data. Incorporating behavioral cues, such as the speed, direction, and distance at which pedestrians recognize and adjust their behavior (e.g., slowing down), could also help account for social relationships between pedestrians. Additionally, this study does not incorporate direct subjective validation methods, such as surveys or interviews, to measure pedestrians' perceived psychological safety. Future studies could address this by combining objective metrics with subjective data, such as analyzing pedestrians' self-reported feelings of safety in specific scenarios. Moreover, as alleyways are frequently used by other types of vehicles beyond cars and pedestrians—such as motorcycles, electric scooters, and shared bicycles—future work could refine the calculation of pedestrian congestion and safety by incorporating the trajectories of these personal mobility devices alongside cars and pedestrians.

Author Contributions: For Conceptualization, Jiyoon Lee; Methodology, Software, Validation, Formal Analysis, Jiyoon Lee; Data Curation, Jiyoon Lee, Youngok Kang; Writing—Original Draft Preparation, Jiyoon Lee; Writing—Review and Editing, Youngok Kang; Visualization, Jiyoon Lee; Supervision, Youngok Kang; Project Administration, Youngok Kang; Funding Acquisition, Youngok Kang. All authors have read and agreed to the published version of the manuscript.

Funding: This research was supported by the Korea Agency for Infrastructure Technology Advancement (KAIA) and funded by the Ministry of Land, Infrastructure, and Transport of the Korean government (Grant No. RS-2022-00143782).

Data Availability Statement: Data can be provided upon request.

Conflicts of Interest: The authors declare no conflicts of interest.

References

1. Edie, L.C. Discussion of traffic stream measurements and definitions. In Proceedings of the 2nd International Symposium on the Theory of Traffic Flow, London, UK, 25–27 June 1963; pp. 139–154.
2. Bansal, P.; Graham, D.J. Congestion in cities: Can road capacity expansions provide a solution? *Transp. Res. Part A Policy Pract.* **2023**, *174*, 103726.
3. Sankaranarayanan, M.; Mala, C.; Jain, S. Traffic density estimation for traffic management applications using neural networks. *Int. J. Intell. Inf. Technol.* **2024**, *20*, 1–19. [CrossRef]
4. Drliciak, M.; Cingel, M.; Celko, J.; Panikova, Z. Research on Vehicle Congestion Group Identification for Evaluation of Traffic Flow Parameters. *Sustainability* **2024**, *16*, 1861. [CrossRef]
5. Munajat, E.; Widyantoro, D.H.; Munir, R. A new method for analyzing congestion levels based on road density and vehicle speed. *J. Theoret. Appl. Inform. Technol* **2017**, *95*, 6454–6471.
6. Feliciani, C.; Nishinari, K. Measurement of congestion and intrinsic risk in pedestrian crowds. *Transp. Res. Part C Emerg. Technol.* **2018**, *91*, 124–155. [CrossRef]
7. Khan, S.D. Congestion detection in pedestrian crowds using oscillation in motion trajectories. *Eng. Appl. Artif. Intell.* **2018**, *85*, 429–443. [CrossRef]
8. Zanlungo, F.; Feliciani, C.; Yucel, Z.; Jia, X.; Nishinari, K.; Kanda, T. A pure number to assess "congestion" in pedestrian crowds. *Transp. Res. Part C Emerg. Technol.* **2023**, *148*, 104041. [CrossRef]
9. Jun, S.U.; Son, Y.T. An Improved LOS Analysis Method for Pedestrian Walkways Using Pedestrian Space. *J. Korean Soc. Transp.* **2016**, *34*, 168–179. [CrossRef]

10. Zhang, P.; Li, X.Y.; Deng, H.Y.; Lin, Z.Y.; Zhang, X.N.; Wong, S.C. Potential field cellular automata model for overcrowded pedestrian flow. *Transp. A Transp. Sci.* **2020**, *16*, 749–775. [CrossRef]
11. Jeong, W.; Oh, H. Study on pedestrian zone widths considering pedestrian density. *Int. J. Highw. Eng.* **2019**, *21*, 73–80. [CrossRef]
12. Jia, X.; Feliciani, C.; Tanida, S.; Yanagisawa, D.; Nishinari, K. Evaluating Pedestrian Congestion Based on Missing Sensing Data. *J. Disaster Res.* **2024**, *19*, 336–346. [CrossRef]
13. Steffen, B.; Seyfried, A. Methods for measuring pedestrian density, flow, speed and direction with minimal scatter. *Phys. A Stat. Mech. Its Appl.* **2010**, *389*, 1902–1910. [CrossRef]
14. Vacková, J.; Bukáček, M. Kernel estimates as general concept for the measuring of pedestrian density. *Transp. A Transp. Sci.* **2023**, 1–26. [CrossRef]
15. Duives, D.C.; Daamen, W.; Hoogendoorn, S.P. Quantification of the level of crowdedness for pedestrian movements. *Phys. A Stat. Mech. Its Appl.* **2015**, *427*, 162–180. [CrossRef]
16. Fruin, J.J. *Pedestrian Planning and Design*; Metropolitan Association of Urban Designers and Environment: New York, NY, USA, 1971.
17. National Academies of Sciences, Engineering, and Medicine. *Highway Capacity Manual Methodologies for Corridors Involving Freeways and Surface Streets*; The National Academies Press: Washington, DC, USA, 2020.
18. Samsung Fire & Marine Insurance Traffic Safety Culture Research Institute. Pedestrian Accident Risk and Prevention Measures in Shared Pedestrian and Vehicle Roads. Samsung Fire & Marine Insurance. 4 April 2019. Available online: https://www.samsungfire.com/vh/page/VH.RNBS0001.do?body=%7B'BBS_ID':'00000071','RTN_KEY':'STSList'%7D (accessed on 2 October 2024).
19. Hall, E.T. *The Hidden Dimension*; Choi, H.S., Translator; Hangilsa Publishing Co., Ltd.: Seoul, Republic of Korea, 2002; pp. 177–195.
20. Ruiz-Perez, M.; Ramos, V.; Alorda-Ladaria, B. Integrating high-frequency data in a GIS environment for pedestrian congestion monitoring. *Inf. Process. Manag.* **2023**, *60*, 103236. [CrossRef]
21. Stock, E.V.; da Silva, R. Exploring crossing times and congestion patterns at scramble intersections in pedestrian dynamics models: A statistical analysis. *Phys. A Stat. Mech. Its Appl.* **2024**, *649*, 129942. [CrossRef]
22. Seoul Metropolitan Government; Whitescan AI Fusion Research Institute; KT AI/BigData Business Division; SKT AD Tech CO.; Shinhan Card Data Biz1 Team. *Seoul Real-Time Urban Data Manual*; Version 5.8; Seoul Metropolitan Government: Seoul, Republic of Korea, 2024.
23. Lee, H.-R.; Lee, J.-M.; Lee, H.-J.; Cho, Y.-N. *A Study on Pedestrian Safety Management Through Analysis of Vulnerable Pedestrian Density Areas in Seoul*; Research Report; Seoul Institute: Seoul, Republic of Korea, 2023; p. 13.
24. Ferrier-Barbut, E.; Vaufreydaz, D.; David, J.A.; Lussereau, J.; Spalanzani, A. Personal space of autonomous car's passengers sitting in the driver's seat. In Proceedings of the 2018 IEEE Intelligent Vehicles Symposium (IV), Suzhou, China, 30 June–1 July 2018; pp. 2022–2029.
25. Dosey, M.A.; Meisels, M. Personal space and self-protection. *J. Personal. Soc. Psychol.* **1969**, *11*, 93–97. [CrossRef]
26. Hayward, J.C. Near miss determination through use of a scale of danger. *Highw. Res. Rec.* **1971**, *384*, 24–34.
27. Hyden, C. Traffic conflicts technique: State-of-the-art. In *Traffic Safety Work with Video-Processing*; Green Series, 43; University Kaiserlauten, Transportation Department: Landau, Germany, 1996; Volume 37, pp. 3–14.
28. Minderhoud, M.M.; Bovy, P.H. Extended time-to-collision measures for road traffic safety assessment. *Accid. Anal. Prev.* **2001**, *33*, 89–97. [CrossRef]
29. Wessels, M.; Oberfeld, D. A binary acceleration signal reduces overestimation in pedestrians' visual time-to-collision estimation for accelerating vehicles. *Heliyon* **2024**, *10*, e27483. [CrossRef]
30. Choi, J.S. *8th Korean Anthropometric Survey Project*; National Institute of Technology and Standards Bio-Chemical Service Standard Division (Size Korea): Eumseong-gun, Republic of Korea, 2021; pp. 92, 132.
31. Kim, E.-C.; Choi, E.-J.; Yang, J.-Y. A Study on Enhancement Methods of Level of Service Analysis for Pedestrian Sidewalks. *J. Korean Soc. Transp.* **2015**, *33*, 29–39. [CrossRef]
32. Lin, L.; Moudon, A.V. Objective versus subjective measures of the built environment, which are most effective in capturing associations with walking? *Health Place* **2010**, *16*, 339–348. [CrossRef]
33. Ministry of Land, Infrastructure and Transport. *Highway Capacity Manual*; Ministry of Land, Infrastructure and Transport: Sejong, Republic of Korea, 2013; pp. 612–637.
34. Kim, T.K. T test as a parametric statistic. *Korean J. Anesthesiol.* **2015**, *68*, 540–546. [CrossRef] [PubMed]
35. Wilcox, R.R. *Kolmogorov-Smirnov Test, Encyclopedia of Biostatistics*; John Wiley & Sons, Ltd.: Hoboken, NJ, USA, 2005.
36. Bland, J.M.; Altman, D. Statistical methods for assessing agreement between two methods of clinical measurement. *Lancet* **1986**, *327*, 307–310. [CrossRef]
37. Myles, P.S.; Cui, J. Using the Bland–Altman method to measure agreement with repeated measures. *Br. J. Anaesth.* **2007**, *99*, 309–311. [CrossRef] [PubMed]

Disclaimer/Publisher's Note: The statements, opinions and data contained in all publications are solely those of the individual author(s) and contributor(s) and not of MDPI and/or the editor(s). MDPI and/or the editor(s) disclaim responsibility for any injury to people or property resulting from any ideas, methods, instructions or products referred to in the content.